ACS APPLIED MATERIALS & INTERFACES

Research Article

www.acsami.org

Correlation between the Length Reduction of Carbon Nanotubes and the Electrical Percolation Threshold of Melt Compounded Polyolefin Composites

Alexandros A. Vasileiou, Marianna Kontopoulou,* Hua Gui, and Aristides Docoslis

Department of Chemical Engineering, Queen's University, Kingston, Ontario K7L 3N6, Canada

ABSTRACT: The objectives of this work are to quantify the degree of multiwalled carbon nanotube (MWCNT) length reduction upon melt compounding and to demonstrate unambiguously that the length reduction is mainly responsible for the increase in electrical percolation threshold of the resulting composites. Polyolefin matrices of varying viscosities and different functional groups are melt compounded with MWCNTs. A simple method is developed to solubilize the polymer matrix and isolate the MWCNTs, enabling detailed imaging analysis. In spite of the perceived strength of the MWCNTs, the results demonstrate that the shear forces developed during melt mixing are sufficient to cause significant nanotube breakage and length reduction. Breakage is promoted when higher MWCNT contents are used, due to increased probability of particle collisions. Furthermore, the higher shear forces transmitted to the nanotubes in the presence of higher matrix viscosities and functional groups that promote interfacial interactions, shift the nanotube distribution toward smaller sizes. The length reduction of the MWCNTs causes significant increases in the percolation threshold, due to the loss of interconnectivity, which results in fewer conductive pathways. These findings are validated by comparing the experimental percolation threshold values with those predicted by the improved interparticle distance theoretical model.

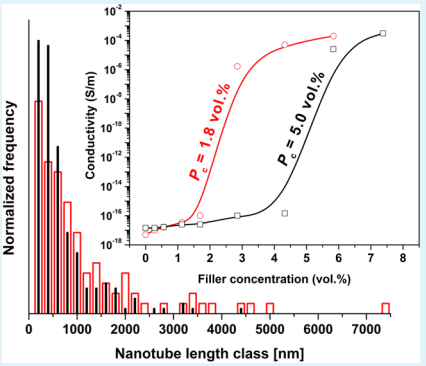

KEYWORDS: *multiwalled carbon nanotubes, melt compounding, length, electrical percolation threshold*

1. INTRODUCTION

The production of polymer/carbon nanotube (CNT) composites by melt compounding has attracted significant attention because it is considered an industrially and economically feasible method.[1−3] However, the large variability on the reported properties of polymer/CNT composites has been a limiting factor for the universal predictability of their performance and will continue to hamper industrial development. As pointed out recently by Verge et al.[4] factors such as the nature and molecular weight of the polymer matrix, the properties of the CNTs, the presence of surface defects, and the melt processing parameters, all dictate the dispersion of the nanotubes, the percolation thresholds, and the final properties of the composites.

CNT dispersion is influenced by the processing conditions, the viscosity of the matrix, and the affinity between the polymer and the filler.[5−11] Higher viscosities, compatibilization, and more intense mixing conditions lead to more efficient primary agglomerate breakup and dispersion due to improved stress transfer to the nanotube aggregates during compounding. The dispersion state, in turn, has a profound effect on the electrical percolation threshold. Generally, low percolation thresholds are achieved when sample-spanning conductive pathways are established within the polymer matrix. It has been shown that this is achieved when aggregates interconnected with individually dispersed nanotubes are present, whereas the absence of a continuous network in well dispersed systems results in higher percolation thresholds.[5,12,13]

The electrical and thermal conductivity of polymer/CNT composites are strongly dominated by the aspect ratio of the nanotubes.[14−20] Shorter lengths result in fewer entanglements and, consequently, a reduction in the size of aggregates.[14,18] Furthermore, it has been demonstrated that carbon nanotubes are subject to breakage during melt compounding[7,12,21,22] when intense mixing conditions and high viscosity matrices are used. It has been speculated that length reduction of the CNT could be a major factor behind the improved dispersion and higher electrical percolation thresholds.

We have recently shown that increased viscosity and noncovalent compatibilization resulted in improved filler dispersion and higher percolation thresholds in linear-low density polyethylene (LLDPE)/multiwalled carbon nanotube (MWCNT) composites.[5] However, it is also plausible that MWCNT breakage could be a major factor behind the improved dispersion and higher electrical percolation thresholds observed. The aim of this study is to clearly address this hypothesis by quantifying the length reduction under well-controlled conditions and to establish correlations with the observed percolation thresholds of the composites. The present

Received: October 16, 2014
Accepted: December 30, 2014
Published: December 30, 2014

DOI: 10.1021/am5071255
ACS Appl. Mater. Interfaces 2015, 7, 1624−1631

study involves polyolefins, which are among the most commonly used polymer matrices in industrial applications.

2. EXPERIMENTAL SECTION

2.1. Materials and Compounding. Multiwalled carbon nanotubes (MWCNTs, purity >95%, diameter 30 ± 15 nm, and length 1−5 μm) were purchased from Nanolab, Inc. (Waltham, MA) and used as received. The specific surface area (SSA) of the nanotubes was 300 m^2/g, as determined by Brunauer−Emmett−Teller (BET) characterization. Engage 8100 and 8130 (named hereafter EOCH and EOCL, respectively), which are poly(ethylene-*co*-octene) copolymers, having MFI of 1.0 g/10 min and 13.0 g/10 min (190 °C/2.16 kg), respectively, with a comonomer content of 38 wt % for EOCH and 42 wt % for EOCL, were obtained from Dow Chemical (Midland, MI). Fusabond E439 (MA), a maleic anhydride grafted LLDPE containing 0.5−1.0 wt % grafts and having a MFI of 2.7 g/10 min (190 °C/2.16 kg), was supplied from E.I. DuPont Canada. LLDPE-*graft*-aminomethylpyridine (PY) was synthesized in a Haake Rheomix E3000 by reacting MA with a molar excess (compared to maleic anhydride grafts) of 4-aminomethylpyridine at 190 °C, as explained in detail by Vasileiou et al.[5] 4-Aminomethylpyridine (AMP, 98% purity) was supplied from Aldrich. All materials and solvents were of analytical grade and were used without further purification.

MWCNTs were melt compounded with MA and PY using a DSM Research 5 mL Micro-Compounder (DSM Resolve, Geleen, Netherlands), at a temperature of 190 °C (60 rpm, 10 min).[5] The EOCH and EOCL composites were prepared at 150 °C (90 rpm, 10 min).[8,23] The detailed preparation and characterization procedures have been reported earlier.[5,8,23] The filler concentration (wt %) of each composite is denoted by the number following the matrix polymer matrix (e.g., for EOCL1 for the EOCL matrix containing 1 wt % MWCNTs). The zero shear viscosities of all the matrices, determined from oscillatory shear tests using a controlled stress rheometer (Viscotech by Reologica) and extrapolated to zero shear, are summarized in Table 1.

Table 1. Zero Shear Viscosities of the Polymer Matrices and Electrical Percolation Threshold Concentrations of Studied Samples

sample	zero shear viscosity[a] (Pa·s)	percolation threshold (vol %)[5,8,23]	percolation threshold (wt %)
EOCL	1100	0.5	1.0
EOCH	14300	1.4	2.6
MA	11100	1.8	3.2
PY	8800	5.0	8.6

[a]At 180 °C for EOCs and 190 °C for LLDPEs.

The volume resistivity of the samples was determined by a Keithley 6517B Electrometer/High Resistance Meter and an Agilent 34401A 6 1/2 Digit multimeter.[5,8,23] Percolation thresholds were determined by fitting the conductivity data, using the following power law relations above and below the critical concentration for percolation[5,8,23]

$$\sigma = \sigma_{matrix}\left(\frac{\varphi_c - \varphi}{\varphi_c}\right)^{-s}, \varphi < \varphi_c \quad (1a)$$

$$\sigma = m\left(\frac{\varphi - \varphi_c}{1 - \varphi_c}\right)^{t} \approx m(\varphi - \varphi_c)^t, \varphi > \varphi_c \quad (1b)$$

where σ is the electrical conductivity of the composite, σ_{matrix} is the conductivity of the matrix, φ is volume fraction of the filler, φ_c is critical volume fraction at percolation, s and t are the critical exponents below and above percolation, respectively, and m is a constant.

2.2. Determination of MWCNT Length Distribution. To isolate MWCNTs from the polymer matrix, the composites were first dissolved in xylene at 110 °C. The solution was filtered dropwise through a nylon membrane with a pore size of 0.1 μm (Sterlitech Corporation, Kent, WA) also at 110 °C to avoid the precipitation of the polymer that could cause filter blockage and/or polymeric residue onto the nanotubes inhibiting transmission electron microscope (TEM) observations. The residue was then washed with copious amounts of hot xylene (110 °C) to ensure complete removal of the polymer. Subsequently, the nanotubes were redispersed in chloroform, which was found to be a suitable solvent for MWCNTs, following a similar methodology as Krause et al.[7] Dispersion was accomplished by immersing the filter in the solvent, with the synchronous application of stirring with a magnetic stirrer and short treatment in an ultrasonication bath for 3 min (Aquasonic 50D, VWR International) to avoid excessive shortening of the MWCNT.[24]

TEM imaging of the as-received and isolated MWCNTs was carried out using a Philips CM 20 electron microscope at an operating voltage of 200 keV. A drop of MWCNTs dispersion in chloroform (0.01 g MWCNTs/L), was placed on a TEM carbon-coated 300 mesh copper grid and dried at ambient temperature prior to analysis. The length of 300 individual MWCNTs was measured using the ImageJ 1.43u image processing program (Wayne Rasband, National Institutes of Health, New York). The full length of each separated nanotube was accounted for, while nanotubes at the edge of the image were excluded. Images were stitched together and were applicable for measuring the length of very long nanotubes. The results are presented as number distributions with class sizes of 200 nm. Length distribution values were quantified by calculating the typical distribution parameters X_{10}, X_{50}, and X_{90}, corresponding to the value where 10, 50, and 90%, respectively, of the nanotubes are smaller.

3. RESULTS

3.1. Method Development. The determination of the length of MWCNTs that are already dispersed within a polymer matrix by conventional imaging is not a trivial matter. Recently, Krause et al. proposed a relatively simple and accurate method to properly determine the length distribution of carbon nanotubes before and after processing.[7] It involves solubilization of the polymer matrix and length distribution analysis from transmission electron microscopy images of the deposited extracted nanotubes. However, this method can only be used reliably in amorphous or low- crystallinity polymers that are readily soluble in chloroform. In the case of polyolefins used in this work, modifications on this method were required. In addition to utilizing hot xylene, which is a suitable solvent for polyolefins, an additional filtration stage was included after the initial solubilization of the composite, followed by redispersion of the isolated nanotubes in chloroform. This allowed for good individualization of the nanotubes and enabled measurements of the length distributions from image analysis of the resulting TEMs. A representative TEM image is shown in Figure 1a. In the absence of this step, aggregated polymer/MWCNT structures were obtained, as shown in Figure 1b, from which it was impossible to discern the dispersed MWCNTs.

3.2. Effect of Concentration. Figure 2 shows an example of the images obtained for the as-received MWCNTs before melt compounding and the corresponding length distributions. The detailed length distributions for all samples before and after melt processing are summarized in Table 2.

Figure 3 and Table 2 clearly show a progressive reduction of the length of the MWCNTs upon compounding of 1.0 and 3.0 wt % MWCNTs with the EOC matrix. As expected, the effect was more pronounced as the CNT content increased. At higher concentrations, there is a higher probability that the MWCNTs will come in contact with each other during compounding, thus increasing the incidence of breakage. At the lower concentration of 1.0 wt % the nanotubes retained 75% of their initial

DOI: 10.1021/am5071255
ACS Appl. Mater. Interfaces 2015, 7, 1624−1631

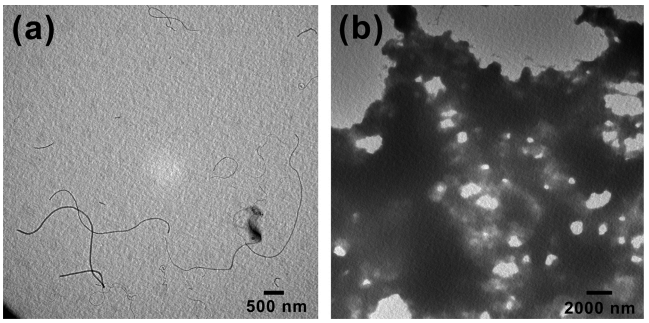

Figure 1. Representative TEM image obtained with (a) modified and (b) established[7] methods for EOCL3.

length, considering X_{50} values, whereas increasing the concentration to 3.0 wt % the retention length was 46%. Furthermore, the significant reduction of the X_{10} value during compounding revealed that breakage led to a higher concentration of very short MWCNTs.

3.3. Effect of Matrix Viscosity. The effect of matrix viscosity on the size distribution of the nanotubes is depicted in Figure 4 and Table 2. The zero shear viscosities of the two EOCs, with high and low viscosities (EOCH and EOCL) are presented in Table 1. A higher matrix viscosity is expected to produce higher shear stresses and mixing energy inputs during compounding, thereby promoting MWCNT dispersion, but also causing breakage. The most severe differences were found in the proportion of long nanotubes, whereas the shorter lengths were not affected significantly by the variation of matrix viscosity. Specifically, the X_{90} values decreased by a further 36% just by the increased melt viscosity. Breakage of the longer MWCNTs resulted in fewer entanglements and, thus, a reduced probability of contacts necessary for electrical conductivity, resulting in significantly higher percolation threshold when the EOCH matrix was used (Table 1).

3.4. Effect of Interfacial Interactions. Our third comparison involved an LLDPE matrix functionalized with aminopyridine (PY), capable of establishing $\pi-\pi$ interactions with the MWCNTs, thus improving stress transfer during compounding compared to its maleated counterpart (MA), which is incapable of such interactions.[5] Upon using this noncovalent compatibilization technique the dispersion of MWCNTs within the PY matrix was significantly improved, owing to the enhanced compatibility between matrix and filler (Figure 5).

Table 2. Distribution Parameters of Length (nm) for As-Received and Recovered from Melt Processed Composites Multi-Walled Carbon Nanotubes

parameter	MWCNT	EOCL1	EOCL3	EOCH3	MA3	PY3
X_{10}	414	250	164	165	150	115
X_{50}	1579	1166	727	558	700	425
X_{90}	4604	3696	2900	2160	2654	1540
$L_{average}$	2220	1995	1200	1050	1190	720

Furthermore, the PY-based composite exhibited narrower MWCNT size distribution, which was shifted to smaller lengths (Figure 6). The nanotubes retained just 44% of their initial length (X_{50} values) when compounded with MA, whereas compounding with PY left only 27% of the initial length. The effect was even more pronounced for the long nanotubes, with a reduction to almost half between X_{90} values of MA and PY (Figure 6). This suggests that enhanced interfacial transfer of shear forces in the presence of aminopyridine functionalization promoted further breakage of the MWCNTs, especially of the long ones. This can be easily attributed to the functionalization procedure only, since the viscosity of the PY matrix was actually lower than that of MA (Table 1).

Noncovalent compatibilization resulted in a significant increase in the percolation threshold to 5 vol %, compared to 1.8 vol % for the MA/MWCNT composites (Table 1 and Figure 7). This may be attributed in part to the improved dispersion of the MWCNTs;[5] however, the results presented herein suggest that nanotube length reduction must also be considered.

To further clarify whether breakage can account for the observed increase in the percolation threshold, we employed the improved interparticle distance (IPD) model, developed by Li et al.,[25] which correlates the length of the MWCNTs with the variation of the percolation threshold concentration. The IPD model contains two dispersion parameters accounting for two extreme cases: (1) all of the cylindrical CNTs are perfectly dispersed in the matrix and (2) all of the CNTs are present in

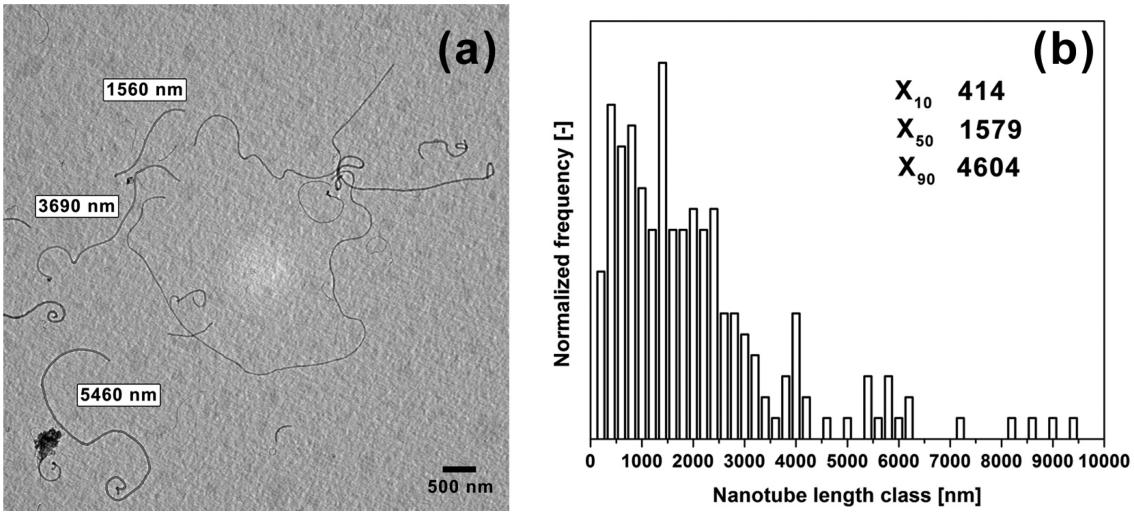

Figure 2. (a) TEM image of as-received MWCNTs with length measurements of the nanotubes and (b) length distribution of MWCNTs.

DOI: 10.1021/am5071255
ACS Appl. Mater. Interfaces 2015, 7, 1624−1631

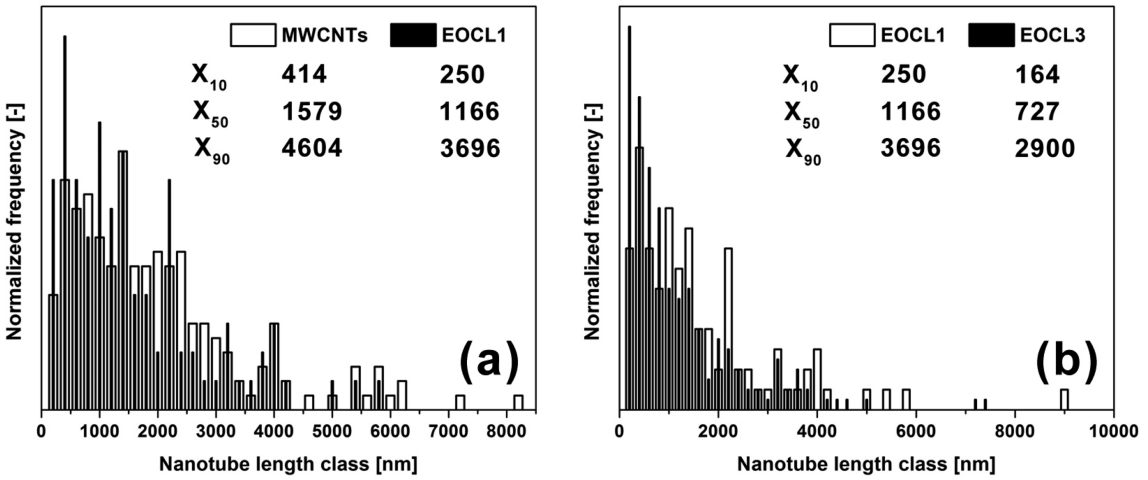

Figure 3. Comparison of length distribution of MWCNTs (a) as-received and recovered from EOCL1 and (b) recovered from EOCL1 and EOCL3.

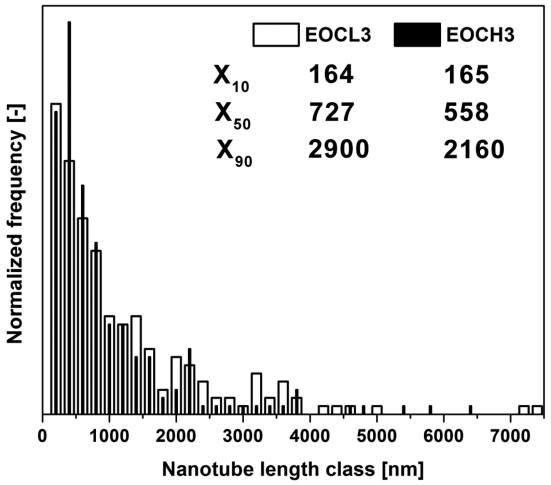

Figure 4. Comparison of length distributions of MWCNTs as recovered from melt processed EOCL3 and EOCH3.

the form of agglomerates. The percolation threshold, P_c, can be calculated using eq 2.

$$P_c = \frac{\xi\varepsilon\pi}{6} + \frac{(1-\xi)27\pi d^2}{4l^2} \quad (2)$$

where ε is the localized volume content of MWCNTs in an agglomerate, ξ is the volume fraction of agglomerated MWCNTs, and d and l are the diameter and length, respectively, of the MWCNTs. A value of $\xi = 0$ represents perfect dispersion of the MWCNTs. As the volume ratio of the agglomerates increases, the percolation threshold becomes more insensitive to the nanotube length, because the first term of eq (1) (length independent part of the model) increases, whereas the second term (length dependent part) decreases proportionally. In the presence of agglomerates ($\xi > 0$) the dependence of the percolation threshold concentration on MWCNT length becomes minimal.

For the purposes of the present analysis perfect dispersion was assumed with no agglomerated MWCNTs present, so that $\xi = 0$. Although this is never the case in real nanocomposites, in which both individual, well-dispersed MWCNTs and MWCNT agglomerates exist, considering such a case presents a scenario in which the length's variation effect on the percolation threshold is maximized. This is actually quite realistic in the PY/MWCNT composites, which contain well-dispersed MWCNTs (Figure 5).

The predictions of the IPD model, obtained using an average nanotube diameter of d = 30 nm are summarized in Table 3 and compared to the experimentally obtained values, which were based on an assumed MWCNT density of 1.65 g/cm^3. The deviations between theoretical predictions and experimental data may be attributed to the assumption of perfect dispersion, the variations in the MWCNT diameter, and the uncertainty in the density of the MWCNTs when estimating the volume fraction.

Upon inspection of the results, it becomes immediately apparent that the length reduction during compounding was the major contributor to the significant increase of the percolation threshold in the PY composites. Taking into account the reduction of the average length alone was sufficient

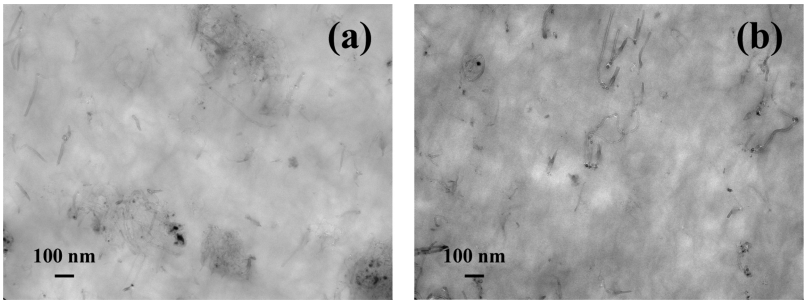

Figure 5. TEM images of (a) MA and (b) PY containing 3.0 wt % MWCNTs.

DOI: 10.1021/am5071255
ACS Appl. Mater. Interfaces 2015, 7, 1624−1631

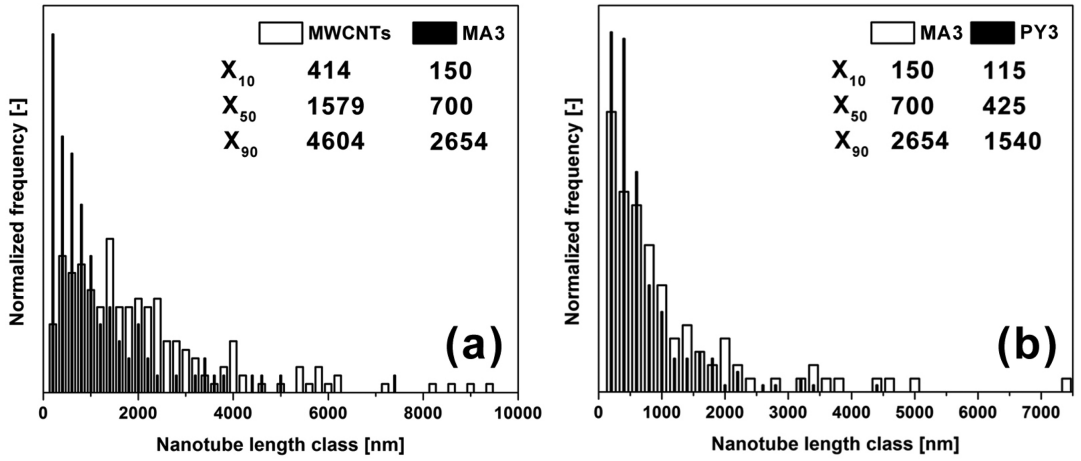

Figure 6. Comparison of length distribution of MWCNTs (a) as received and recovered from MA3 and (b) recovered from MA3 and PY3.

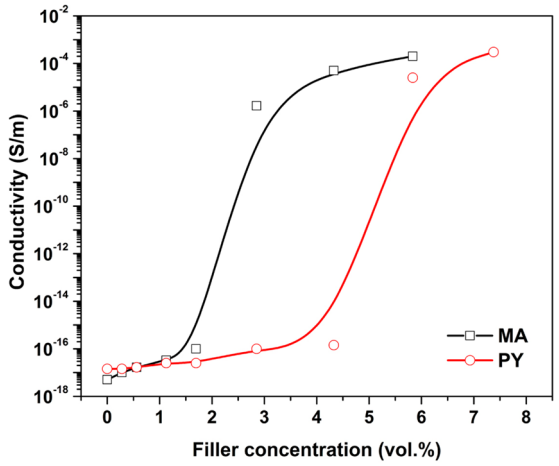

Figure 7. Electrical conductivity as a function of MWCNT concentration. Solid lines denote fits obtained using eqs 1a and 1b.

Table 3. Percolation Threshold Concentration Based on IPD Model.[25]

sample	$L_{average}$ (nm)	experimental (vol %)	IPD model (vol %)
MA3	1190	1.8	1.3
PY3	720	5.0	3.7

to predict a 3-fold increase in the percolation threshold concentration (Table 3). This is similar in magnitude with the increase observed experimentally. Therefore, the significant loss of length is the main contributing factor in the increase in electrical percolation threshold concentrations in the PY composite.

The small discrepancies between the experimental and the predicted results can be attributed to the presence of polymer that is physically adsorbed on the surface of the nanotubes. This would be more pronounced in the case of the PY composites, which have enhanced interfacial interactions. The presence of even small amounts of adsorbed polymer hinders direct contact between nanotubes, thus inhibiting the formation of a conducting network and consequently increasing the percolation threshold. The IPD model, which accounts only for the contacts between nanotubes, without taking the presence of adsorbed polymer into account would therefore predict a lower percolation threshold. The physically absorbed polymer may further act as a tunneling barrier between the filler particles resulting in significantly lower than expected composite conductivities (Figure 7),[26] compared to the properties of the neat nanotubes.[27]

4. DISCUSSION

It has been noted extensively in the literature that filler dispersion and the electrical and mechanical properties of polymer/MWCNT composites are ultimately related to the length of the nanotubes[14−20,28] and, more specifically, in the case of melt compounding, to the residual MWCNT length inside the polymer matrix. Our results, summarized in Table 2 and Figure 8, show a significant shift in the size distribution of

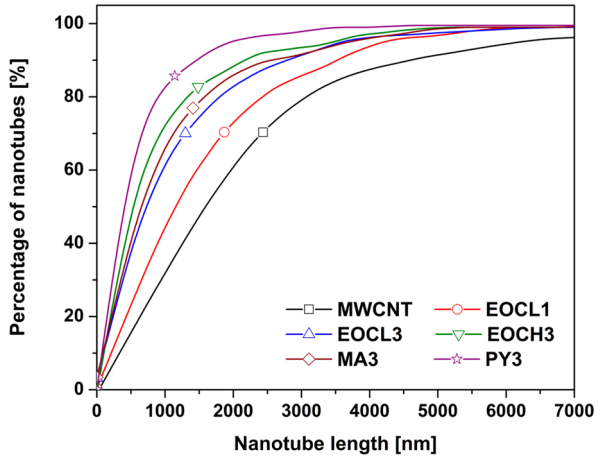

Figure 8. Comparison of cumulative length distribution curves of pure and recovered from melt processed composites multiwalled carbon nanotubes.

the MWCNTs upon melt compounding, which becomes more pronounced at higher filler contents, due to the increased probability of collisions and fracture of the nanotubes. A clear trend toward shorter nanotubes is also seen as the viscosity increases and in compatibilized formulations, which promote improved interfacial interactions. While nanotube length reduction upon melt compounding has been reported before for composites based on polycarbonate and polystyrene,[12,22,29] it is the first time that nanotube breakage is quantified and reported in polyolefins, while considering simultaneously the

DOI: 10.1021/am5071255
ACS Appl. Mater. Interfaces 2015, 7, 1624−1631

contribution of factors such as filler concentration, matrix viscosity, and interfacial interactions. This confirms that CNT breakage is a widespread phenomenon during melt compounding of composites based on thermoplastic matrixes.

We have also demonstrated that shortening of the MWCNTs promotes disentanglement and improves dispersion within polyolefin matrixes, resulting ultimately in higher percolation thresholds, due to a loss in interconnectivity. Therefore, the effects of length reduction during processing should always be considered when trying to control the percolation thresholds. The ability to control the MWCNT length appears to be extremely important to attain the high electrical and physical performance of polymer/MWCNT composites predicted by theoretical studies.

Even though it is widely accepted that MWCNTs have remarkable mechanical properties, it has been demonstrated that external forces by ultrasound[20,24,30,31] and ball milling[14,18,30,32] can cause breakage. Our work clearly demonstrates that shear forces developed during melt mixing are also sufficient to fracture the nanotubes and reduce their lengths.

It is well documented that fibers, including the commonly used carbon fibers and glass fibers, are easily broken by external forces exerted on them during processing,[33] due to a mechanism of bending and buckling during shear flow.[34] Pagani et al.[24] suggested that these mechanisms are also responsible for the breakage of CNTs and that longer CNTs are especially susceptible to buckling, with axial buckling being dominant. Buckling occurs when the fluid shear stress is higher than the buckling stress (σ_b), calculated by the following equation:[34]

$$\sigma_b = \frac{E_f\left[\ln\left(\frac{l}{d}\right) - 1.75\right]}{2\left(\frac{l}{d}\right)^4} \quad (3)$$

where E_f is the Young's modulus, and l and d are the length and diameter, respectively, of the filler. Assuming values of tensile strength of 3.6 GPa and Young's modulus of 0.450 TPa[35] for commercial carbon nanotubes prepared by carbon vapor deposition (CVD) and values of d = 0.03 μm and l = 2.22 μm ($L_{average}$), a shear stress of the order of 20 kPa is calculated for buckling. Shear forces of the order of MPa are typically encountered during regular melt compounding operations, which are much larger than σ_b and therefore significant buckling of the CNTs will take place during compounding.

Once buckled, a CNT must experience a sufficiently high local curvature stress to break. This happens at a critical radius of curvature, R_b, which can be determined from thin rod theory according to the equation:[24,34]

$$\frac{R_b}{d} = \frac{E_f}{2\sigma_f} \quad (4)$$

where σ_f is the tensile strength of the filler. For a rod-shaped filler, the higher the value of R_b, the less bending is needed to cause breakage. Furthermore, decreasing aspect ratio as a result of breakage leads to increased σ_b, with shorter nanotubes being more difficult to break and, thus, a limiting value of fiber length is eventually reached.

Using the typical CNT length and diameter values mentioned above, a value of R_b = 1.88 μm was obtained, which is close to the average length of the nanotubes. The values obtained by applying eqs 3 and 4 suggest that the nanotubes used in this work are very likely to break because the shear forces during compounding are much higher than σ_b, while the degree of bending needed to induce breakage is relatively low and of the same order of magnitude to the average nanotube length.

In addition to the considerations mentioned above, the situation encountered in MWCNTs is more complicated than what is reported in common fibers. MWCNT consist of cylindrical layers. The loads (shear, tension, compression) would be transferred by the polymer matrix to the MWCNTs via the nanotube/matrix interface and from the outermost layer and into the inner layers. Given that the cylindrical layers are bonded weakly through van der Waals interactions, the MWCNTs are susceptible to interlayer forces,[36] resulting in highly anisotropic stresses, which may lead to fracture.

Another reason for the susceptibility of MWCNTs to breakage is the existence of defects and heterogeneities at the nanoscale.[37−39] Defects such as vacancies, metastable atoms, pentagons, Stone−Wales defects, heterogeneous atoms, and discontinuities of walls are widely exhibited by as much as 10% of the nanotubes in commercial MWCNT samples. These defects play an important role in the mechanical, electrical, chemical and other properties of the carbon nanotubes. Mechanical stimuli can cause the formation of further defects, beyond certain values of strain that are as low as 5−6%.[40] High defect densities and geometrical irregularities in mass-produced MWCNTs can degrade mechanical properties, such as tensile strength, down to 60% of the intact tube.[41] Considering the effect of the tensile strength values in eqs 3 and 4, it is a straightforward conclusion that MWCNTs fracture becomes easier than what would be expected considering their ideal properties.

Given that residual MWCNT length plays such an important role in determining the properties of the composites, prevention of breakage and length retention are important issues that must be addressed to achieve the highest performance from the composites. However, sufficient, reproducible, and effective control of the structural quality of MWCNTs still remains a challenge.[42] Improvements in the synthetic procedure of MWCNTs leading to reduction and uniformity of structural defects would help retain the initial length in the composite and give rise to improved composites with more predictable properties, enabling them to become industrial commodities.

5. SUMMARY

A simple method involving solubilization of the polyolefin matrix and the isolation and purification of the nanotubes followed by length distribution analysis using TEM, was implemented to accurately measure the length distribution of MWCNTs in polyolefinic composites. The statistical analysis revealed a progressive reduction of the length of MWCNTs upon melt compounding. Breakage led to a significant increase in the number of very short MWCNTs and a narrowing of the length distribution. As the MWCNT concentration increased, so did the probability of particle−particle collisions, resulting in further length reductions. Increasing the matrix viscosity facilitated MWCNT dispersion at the cost of residual length, especially of the long nanotubes. This led to increased percolation threshold. Noncovalent compatibilization also improved the dispersion significantly, due to enhanced interfacial interactions between the matrix and the nanotubes. However, interfacial stress transfer promoted breakage, resulting in a significant decrease in the length distribution of

DOI: 10.1021/am5071255
ACS Appl. Mater. Interfaces 2015, 7, 1624−1631

the MWCNT, to almost half compared to the noncompatibilized composite. The combined result was that the electrical percolation thresholds were significantly increased due to a loss in interconnectivity in the presence of shorter nanotubes. Application of the IPD theoretical model to correlate the length of the nanotubes with the percolation threshold confirmed that the increased percolation threshold concentrations were attributed mainly to the breakage and shortening of the nanotubes.

AUTHOR INFORMATION

Corresponding Author

*E-mail: kontopm@queensu.ca.

Notes

The authors declare no competing financial interest.

ACKNOWLEDGMENTS

Financial support from the Natural Sciences and Engineering Research Council of Canada (NSERC) through the Discovery and Accelerator Supplement programs is gratefully acknowledged. The polymers used in this study were donated by E.I. DuPont Canada and Dow Chemical.

REFERENCES

(1) Song, K.; Zhang, Y.; Meng, J.; Green, E.; Tajaddod, N. Structural Polymer-Based Carbon Nanotube Composite Fibers: Understanding the Processing−Structure−Performance Relationship. *Materials* **2013**, *6*, 2543−2577.

(2) De Volder, M. F. L.; Tawfick, S. H.; Baughman, R. H.; Hart, A. J. Carbon Nanotubes: Present and Future Commercial Applications. *Science* **2013**, *339*, 535−539.

(3) Han, Z.; Fina, A. Thermal Conductivity of Carbon Nanotubes and their Polymer Nanocomposites: A Review. *Prog. Polym. Sci.* **2011**, *36*, 914−944.

(4) Verge, P.; Benali, S.; Bonnaud, L.; Minoia, A.; Mainil, M.; Lazzaroni, R.; Dubois, P. Unpredictable dispersion states of MWNTs in HDPE: A Comparative and Comprehensive Study. *Eur. Polym. J.* **2012**, *48*, 677−683.

(5) Vasileiou, A. A.; Docoslis, A.; Kontopoulou, M.; Xiang, P.; Ye, Z. The Role of Non-Covalent Interactions and Matrix Viscosity on the Dispersion and Properties of LLDPE/MWCNT Nanocomposites. *Polymer* **2013**, *54*, 5230−5240.

(6) Potts, J. R.; Shankar, O.; Du, L.; Ruoff, R. S. Processing-Morphology-Property Relationships and Composite Theory Analysis of Reduced Graphene Oxide/Natural Rubber Nanocomposites. *Macromolecules* **2012**, *45*, 6045−6055.

(7) Krause, B.; Boldt, R.; Pötschke, P. A Method for Determination of Length Distributions of Multiwalled Carbon Nanotubes Before and After Melt Processing. *Carbon* **2011**, *49*, 1243−1247.

(8) Osazuwa, O.; Kontopoulou, M.; Xiang, P.; Ye, Z.; Docoslis, A. Electrically Conducting Polyolefin Composites Containing Electric Field-Aligned Multiwall Carbon Nanotube Structures: The Effects of Process Parameters and Filler Loading. *Carbon* **2014**, *72*, 89−99.

(9) Yuan, W.; Chan-Park, M. B. Covalent Cum Noncovalent Functionalizations of Carbon Nanotubes for Effective Reinforcement of a Solution Cast Composite Film. *ACS Appl. Mater. Interfaces* **2012**, *4*, 2065−2073.

(10) Liao, W.; Tien, H.; Hsiao, S.; Li, S.; Wang, Y.; Huang, Y.; Yang, S.; Ma, C. M.; Wu, Y. Effects of Multiwalled Carbon Nanotubes Functionalization on the Morphology and Mechanical and Thermal Properties of Carbon Fiber/Vinyl Ester Composites. *ACS Appl. Mater. Interfaces* **2013**, *5*, 3975−3982.

(11) Giambastiani, G.; Cicchi, S.; Giannasi, A.; Luconi, L.; Rossin, A.; Mercuri, F.; Bianchini, C.; Brandi, A.; Melucci, M.; Ghini, G.; et al. Functionalization of Multiwalled Carbon Nanotubes with Cyclic Nitrones for Materials and Composites: Addressing the Role of CNT Sidewall Defects. *Chem. Mater.* **2011**, *23*, 1923−1938.

(12) Arjmand, M.; Mahmoodi, M.; Park, S.; Sundararaj, U. An Innovative Method to Reduce the Energy Loss of Conductive Filler/Polymer Composites for Charge Storage Applications. *Compos. Sci. Technol.* **2013**, *78*, 24−29.

(13) Alig, I.; Pötschke, P.; Lellinger, D.; Skipa, T.; Pegel, S.; Kasaliwal, G. R.; Villmow, T. Establishment, Morphology, and Properties of Carbon Nanotube Networks in Polymer Melts. *Polymer* **2012**, *53*, 4−28.

(14) Li, F.; Lu, Y.; Liu, L.; Zhang, L.; Dai, J.; Ma, J. Relations between Carbon Nanotubes' Length and their Composites' Mechanical and Functional Performance. *Polymer* **2013**, *54*, 2158−2165.

(15) Wang, X.; Jiang, Q.; Xu, W.; Cai, W.; Inoue, Y.; Zhu, Y. Effect of Carbon Nanotube Length on Thermal, Electrical, and Mechanical Properties of CNT/Bismaleimide Composites. *Carbon* **2013**, *53*, 145−152.

(16) Singh, I.; Verma, A.; Kaur, I.; Bharadwaj, L. M.; Bhatia, V.; Jain, V. K.; Bhatia, C. S. The Effect of Length of Single-Walled Carbon Nanotubes (SWNTs) on Electrical Properties of Conducting Polymer/SWNT Composites. *J. Polym. Sci., Part B: Polym. Phys.* **2010**, *48*, 89−95.

(17) Bui, K.; Grady, B. P.; Saha, M. C.; Papavassiliou, D. V. Effect of Carbon Nanotube Persistence Length on Heat Transfer in Nanocomposites: A Simulation Approach. *Appl. Phys. Lett.* **2013**, *102*, 203116.

(18) Menzer, K.; Krause, B.; Boldt, R.; Kretzschmar, B.; Weidisch, R.; Pötschke, P. Percolation Behaviour of Multiwalled Carbon Nanotubes of Altered Length and Primary Agglomerate Morphology in Melt Mixed Isotactic Polypropylene-Based Composites. *Compos. Sci. Technol.* **2011**, *71*, 1936−1943.

(19) Shokrieh, M. M.; Rafiee, R. Investigation of Nanotube Length Effect on the Reinforcement Efficiency in Carbon Nanotube Based Composites. *Compos. Struct.* **2010**, *92*, 2415−2420.

(20) Russ, M.; Rahatekar, S. S.; Koziol, K.; Farmer, B.; Peng, H.-X. Length-Dependent Electrical and Thermal Properties of Carbon Nanotube-Loaded Epoxy Nanocomposites. *Compos. Sci. Technol.* **2013**, *81*, 42−47.

(21) Fu, S. Y.; Chen, Z.-K.; Hong, S.; Han, C. C. The Reduction of Carbon Nanotube (CNT) Length During the Manufacture of CNT/Polymer Composites and a Method to Simultaneously Determine the Resulting CNT and Interfacial Strengths. *Carbon* **2009**, *47*, 3192−3200.

(22) Socher, R.; Krause, B.; Müller, M. T.; Boldt, R.; Pötschke, P. The Influence of Matrix Viscosity on MWCNT Dispersion and Electrical Properties in Different Thermoplastic Nanocomposites. *Polymer* **2012**, *53*, 495−504.

(23) Osazuwa, O.; Petrie, K.; Kontopoulou, M.; Xiang, P.; Ye, Z.; Docoslis, A. Characterization of Non-Covalently, Non-Specifically Functionalized Multi-Wall Carbon Nanotubes and Their Melt Compounded Composites with an Ethylene−Octene Copolymer. *Compos. Sci. Technol.* **2012**, *73*, 27−33.

(24) Pagani, G.; Green, M. J.; Poulin, P.; Pasquali, M. Competing Mechanisms and Scaling Laws for Carbon Nanotube Scission by Ultrasonication. *Proc. Natl. Acad. Sci. U.S.A.* **2012**, *109*, 11599−11604.

(25) Li, J.; Ma, P. C.; Chow, W. S.; To, C. K.; Tang, B. Z.; Kim, J.-K. Correlations between Percolation Threshold, Dispersion State, and Aspect Ratio of Carbon Nanotubes. *Adv. Funct. Mater.* **2007**, *17*, 3207−3215.

(26) McNally, T.; Pötschke, P.; Halley, P.; Murphy, M.; Martin, D.; Bell, S. E. J.; Brennan, G. P.; Bein, D.; Lemoine, P.; Quinn, J. P. Polyethylene Multiwalled Carbon Nanotube Composites. *Polymer* **2005**, *46*, 8222−8232.

(27) Bauhofer, W.; Kovacs, J. Z. A Review and Analysis of Electrical Percolation in Carbon Nanotube Polymer Composites. *Compos. Sci. Technol.* **2009**, *69*, 1486−1498.

(28) Deng, L.; Eichhorn, S. J.; Kao, C.; Young, R. J. The Effective Young's Modulus of Carbon Nanotubes in Composites. *ACS Appl. Mater. Interfaces* **2011**, *3*, 433−440.

DOI: 10.1021/am5071255
ACS Appl. Mater. Interfaces 2015, 7, 1624−1631

(29) Guo, J.; Liu, Y.; Prada-Silvy, R.; Tan, Y.; Azad, S.; Krause, B.; Pötschke, P.; Grady, B. P. Aspect Ratio Effects of Multi-Walled Carbon Nanotubes on Electrical, Mechanical, and Thermal Properties of Polycarbonate/MWCNT Composites. *J. Polym. Sci., Part B: Polym. Phys.* **2014**, *52*, 73−83.
(30) Chowdhury, D. F.; Cui, Z. F. Carbon Nanotube Length Reduction Techniques, and Characterisation of Oxidation State using Quasi-Elastic Light Scattering. *Carbon* **2010**, *49*, 862−868.
(31) Inam, F.; Vo, T.; Jones, J. P.; Lee, X. Effect of Carbon Nanotube Lengths on the Mechanical Properties of Epoxy Resin: An Experimental Study. *J. Compos. Mater.* **2012**, *47*, 2321−2330.
(32) Krause, B.; Villmow, T.; Boldt, R.; Mende, M.; Petzold, G.; Pötschke, P. Influence of Dry Grinding in a Ball Mill on the Length of Multiwalled Carbon Nanotubes and their Dispersion and Percolation Behaviour in Melt Mixed Polycarbonate Composites. *Compos. Sci. Technol.* **2011**, *71*, 1145−1153.
(33) Fu, S.-Y.; Lauke, B.; Mai, Y. W. *Science and Engineering of Short Fibre Reinforced Polymers Composites*; CRC Press: Boca Raton, FL, 2009.
(34) Ville, J.; Inceoglu, F.; Ghamri, N.; Pradel, J. L.; Durin, A.; Valette, R.; Vergnes, B. A Study of Fiber Breakage during Compounding in a Buss Kneader. *Int. Polym. Process* **2012**, *27*, 245−251.
(35) Xie, S.; Li, W.; Pan, Z.; Chang, B.; Sun, L. Mechanical and Physical Properties on Carbon Nanotube. *J. Phys. Chem. Solids* **2000**, *61*, 1153−1158.
(36) Viet, N. V.; Kuo, W. S. Shear Transfer in Fractured Carbon Nanotubes under Torsion. *Mater. Sci. Eng., A* **2012**, *536*, 256−264.
(37) Yuan, Q.; Xu, Z.; Yakobson, B. I.; Ding, F. Efficient Defect Healing in Catalytic Carbon Nanotube Growth. *Phys. Rev. Lett.* **2012**, *108*, 245505.
(38) Yoshida, H.; Takeda, S. Elucidation of the Origin of Grown-in Defects in Carbon Nanotubes. *Carbon* **2014**, *70*, 266−272.
(39) Saidi, W. a.; Norman, P. Probing Single-Walled Carbon Nanotube Defect Chemistry using Resonance Raman Spectroscopy. *Carbon* **2014**, *67*, 17−26.
(40) Lu, Q.; Bhattacharya, B. Effect of Randomly Occurring Stone−Wales Defects on Mechanical Properties of Carbon Nanotubes using Atomistic Simulation. *Nanotechnology* **2005**, *16*, 555−566.
(41) Sammalkorpi, M.; Krasheninnikov, A.; Kuronen, A.; Nordlund, K.; Kaski, K. Mechanical Properties of Carbon Nanotubes with Vacancies and Related Defects. *Phys. Rev. B* **2004**, *70*, 245416.
(42) Choi, J.; Pyo, S.; Baek, D.-H.; Lee, J.-I.; Kim, J. Thickness-, Alignment- and Defect-Tunable Growth of Carbon Nanotube Arrays using Designed Mechanical Loads. *Carbon* **2014**, *66*, 126−133.

DOI: 10.1021/am5071255
ACS Appl. Mater. Interfaces 2015, 7, 1624−1631